JOURNAL OF MATERIALS SCIENCE 12 (1977) 277–289

# Optimization of the three-point bend test for fracture energy measurement

G. A. COOPER
*Institut CERAC S.A., Chemin des Larges-Pièces, CH-1024 Ecublens, Switzerland*

Of the various methods for measuring the fracture energy of a material, the three-point slow bend test has the merit of being simple and straightforward to execute. It can only be expected to give valid results, however, when the crack propagates quasi-statically. A simple criterion is proposed to determine whether a specimen of given geometry and meterial will fracture in a stable or unstable manner when tested in a particular machine. The prediction of the criterion is compared with experimental results obtained on a variety of rocks, and is found to give good agreement.

## 1. Introduction

The fracture energy of a material may be obtained either by measuring stresses or loads during fracture, or by measuring the consumption of energy by the growing crack. These two approaches may be again subdivided according to whether they are applied to the initiation of crack growth, or to the steady state. In principle, any specimen geometry may be used, provided that either the stress-intensity factor, $K$, or the strain energy release rate can be determined, and provided that the conditions of crack growth correspond to those of interest for the ulterior use of the information.

In practice, most of the methods based on the measurement of stresses or loads are applied to the initiation of crack growth, whereas the energy methods are more often concerned with its propagation. In general, the former are of more interest to the designer concerned with the load-carrying ability of a structure, for once a crack has begun to propagate, the structure is never again as strong, and it can be considered to have failed. Measurements of the steady-state fracture energy, on the other hand, are of use when making estimates of the energy required to complete the fracture. Such values are useful, for example, in estimating the energy-absorbing ability of a structure loaded under crash conditions or, in the case of our laboratory, in estimating the energy requirement for a machine to excavate a certain quantity of rock.

Within the group of energy methods, there are both dynamic and static techniques. The former include the Charpy and Izod tests, which, while they have been successfully applied to ceramics and other brittle materials [1], must be treated with some caution; Marshall *et al.* [2]. have pointed out that the kinetic energy imparted to the broken pieces of the specimen is comparable with the fracture energy of many ceramics, and it must be accurately measured and deducted in calculating the fracture energy.

In the quasi-static regime, the slow bend test is pre-eminent (and is the main subject of this report). This test was developed independently by Tattersall and Tappin [3, 4] and Nakayama [5]. The technique consists of taking a notched beam and breaking it in three- or four-point bending. If the test is correctly arranged, the fracture can be started and propagated to failure in a quasi-static manner, with the applied load always equal to that necessary to just maintain growth of the crack. Since, at the beginning and at the end of the test, the loads are everywhere zero, the integral of the force-displacement curve of the test machine between these two conditions must be equal the energy consumed in producing the new fracture surfaces. A particular advantage of this and other energy methods arises since one obtains

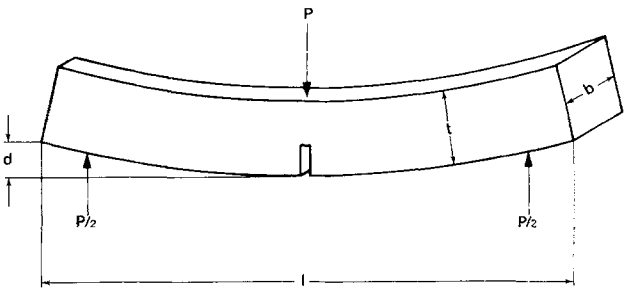


*Figure 1* The three-point beam test.

an average value of the fracture energy for the whole cross-section of the specimen. This is particularly useful in dealing with a material as variable as rock.

The success of the method depends upon always having a quantity of stored elastic energy in the beam and loading system which is less than that necessary to complete the fracture. In practice, this amounts to ensuring that the loading system is sufficiently stiff, and to providing a suitable starting notch which causes the crack to start growth at a sufficiently small load.

## 2. The present approach

We have examined the energy balance in the machine and specimen at the onset of fracture, in order to determine the various parameters which govern the stability of the fracture process.

We consider a rectangular beam, loaded in three-point bending, and shall examine the energy balance in the beam at the moment of incipient fracture (Fig. 1). This is taken to be the moment at which the applied load reaches a maximum, and so, therefore, does the stored elastic energy in the system. If this energy is less than that necessary to generate the new surfaces when the beam breaks, the fracture will be considered to be stable.

The stored elastic energy in the beam is:

$$Q_B = \int_{\sigma=0}^{\sigma_{max}} P \mathrm{d}(d)$$

where $P$ is the load applied by the testing machine, $d$ is the beam centre point deflection, and $\sigma$ is the fibre tensile stress in the beam at the point of incipient failure. If the beam is considered to be long and thin*,

$$Q_B = \int_{\sigma=0}^{\sigma_{max}} \frac{4Ebt^3}{l^3} \mathrm{d}(d) \qquad (1)$$

where $E$ is the Young's modulus, and $b$, $t$ and $l$ are the beam dimensions. At incipient fracture, $\sigma$ reaches $\sigma_{max}$, the modulus of rupture. In an unnotched beam, this is related to the failure load by the expression

$$\sigma_{max} = \frac{3Pl}{2bt^2}.$$

If the beam is notched, failure will occur at a lower load, due to the stress concentration introduced by the notch. The stress-concentration factor, $S$, can be calculated analytically for certain geometries of beam and notch (see, for example, [6] and [7]). Alternatively, it can be obtained by simply making a test on a beam of the desired shape: it is not necessary that the fracture be stable since all that is required is the failure load.

At the maximum load, then,

$$P_{max} = \frac{2bt^2 \sigma_{max}}{3lS}$$

and

$$d = \frac{l^3}{4Ebt^3} \cdot \frac{2bt^2 \sigma_{max}}{3lS}.$$

Equation 1 thus becomes:

$$Q_B = \left[\frac{2Ebt^3 d^2}{l^3}\right]_{d=0}^{\frac{l^2 \sigma_{max}}{6EtS}}$$

$$= \frac{1}{18} \cdot \frac{\sigma_{max}^2 l bt}{ES^2}. \qquad (2)$$

The stored energy in the testing machine at the moment of failure may be found similarly:

*This expression ignores the contribution to the stored elastic energy from the shear deformation and also the decrease in the stiffness of the beam caused by the presence of the notch. The former will be small if the beam is long, and the latter will be small if the notch itself is narrow. In this simplified treatment we have chosen to adopt a phenomenological approach, and to include this contribution implicitly in the factor $S$. Alternatively, for certain geometries, the stored energy in the beam can be calculated completely, and a stability criterion can also be obtained from this starting point [11].

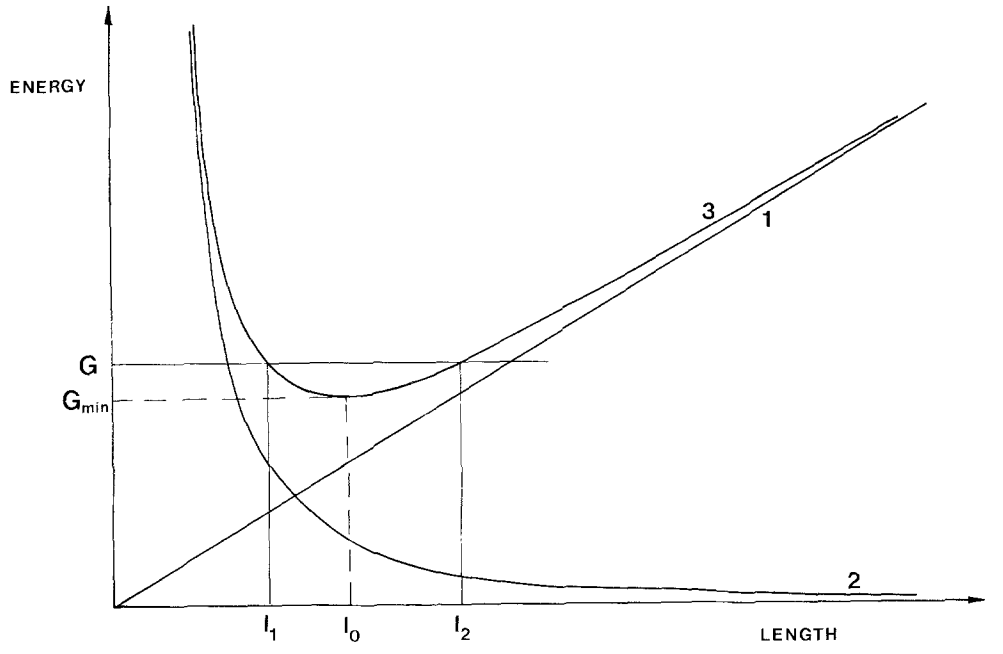


*Figure 2* The variation of stored energy per unit area of fracture surface as a function of beam length; (1) beam energy, (2) energy stored in the machine, (3) total energy.

$$Q_m = \int_{P=0}^{P_{max}} P\,dx$$

where $x$ is the elastic deflection of the testing machine. If the machine stiffness is defined as $S_m$, we have $S_m = P/x$ and $dx = dP/S_m$. Thus

$$Q_m = \int_{P=0}^{P_{max}} \frac{P\,dP}{S_m}.$$

Now

$$P_{max} = \frac{2bt^2\sigma_{max}}{3lS}$$

so

$$Q_m = \left[\frac{P^2}{2S_m}\right]_{P=0}^{\frac{2bt^2\sigma_{max}}{3lS}}$$

$$= \frac{1}{2S}\left(\frac{2bt^2\sigma_{max}}{3lS}\right)^2. \qquad (3)$$

For stable fracture to occur, the sum of the stored energies $Q_B$ and $Q_m$ should be less than the energy required to form the crack which causes the fracture of the beam.

For stability,

$$GA \geqslant Q_m + Q_B \qquad (4)$$

where $A$ is the area to be broken ($A$ is the area over which the crack front passes, creating two new surfaces, each of area $A$. This convention requires that $G$ be the analogue of $2\gamma$, as is usual). In the particular geometry under consideration, with the notch cut so as to leave a bridge in the form of an isosceles triangle, the bridge area is $bt/2$. Criterion 4 thus becomes:

$$G \geqslant \frac{\sigma_{max}^2}{9S^2}\left(\frac{l}{E} + \frac{4bt^3}{S_m l^2}\right) \qquad (5)$$

The physical significance of the criterion can be easily appreciated by reference to Fig. 2, in which the contributions to the stored energy by the two terms on the right-hand side of Equation 5 are shown as a function of beam length. The first term (curve 1) is proportional to $l$, and represents the energy stored in the beam. The second term (curve 2), inversely proportional to $l^2$, represents the energy stored in the testing machine. The sum of these two terms (curve 3) must be less than $G$ to ensure stable fracture. This is seen to occur between $l_1$ and $l_2$, and, in general, stable fractures will be found for beam lengths between two such limits. For very short beams, the failure load is high, and this causes too much energy to be stored in the testing machine, although the energy stored in the beam is small. Conversely, for very long beams, although the failure load is now low, the beam is so flexible that it stores enough energy in

its own elastic deformation to ensure an unstable fracture. It is of course possible that for very brittle materials, the minimum value of the stored energy from both sources is never sufficiently low to be below $G$, and for stable fractures to be produced. This value can be conveniently found from Equation 5, by differentiating with respect to $l$, and equating to zero. Whence

$$l_0 = \left(\frac{8bt^3E}{S_m}\right)^{1/3}$$

and re-substituting in Equation 5 the minimum value of $G$ for which stable fracture can be obtained is found as:

$$G_{min} = \frac{\sigma_{max}^2}{9S^2}\left[\left(\frac{8bt^3}{E^2S_m}\right)^{1/3} + \left(\frac{b}{S_m E^2}\right)^{1/3}\right]. \quad (6)$$

To obtain stable fractures with materials more brittle than this, it is necessary to alter other variables, e.g. by increasing the severity of the notch, or by increasing the stiffness of the testing machine.

Equation 6 can be conveniently cast in the form of three dimensionless groups: stability is obtained when:

$$\frac{P^2l^3}{4EGb^2t^4} + \frac{P^2}{S_m Gbt} \leqslant 1 \quad (A)$$

or when

$$\frac{GbtS_m}{P^2} - \frac{l^3S_m}{4Ebt^3} \geqslant 1 \quad (B)$$

or when

$$\frac{4GEb^2t^4}{P^2l^3} - \frac{4Ebt^3}{S_m l^3} \geqslant 1. \quad (C)$$

Use of these forms should thus enable an evaluation of the stability criterion to be made, independent of machine and material variations. The following parts of this report, covering the experimental work, are largely concerned with this evaluation.

## 3. Experimental work

The work described below covers the experiments necessary for testing of the stability criterion developed above, the investigation of possible scaling effects, and the measurement of fracture energies for a variety of rocks. They will be described here in the above order, although in fact this was not the order in which the experiments were performed. For example, before proceeding to the testing of the theory, it was necessary to investigate possible size effects in order to determine a convenient size of test specimen which would be unaffected by this variable. This was suspected, since Hoagland *et al.* [8, 9] have shown that there is considerable evidence that the crack must run up to several millimetres before the distribution of microcracks in the region of the crack tip has reached an equilibrium state.

Experiments were carried out on the following rocks: marble, from Carrara, Italy, and Lasa, Switzerland; granite from Bohus, Sweden, and Miéville, Switzerland; sandstone (grey flysch types) from Alpnach and Val d'Illiez, both Switzerland, and the well-knowm compact, lithographic quality limestone from Solnhofen (Germany). This choice is representative of a wide variety of rock types, in origin (igneous, metamorphic and sedimentary), in chemical composition, and in grain size.

### 3.1. The stability criterion

Testing was carried out on an Instron 10 000 kg testing machine (Model 1215), in three-point bend, on notched rectangular beams of various dimensions. The notches were cut with a diamond saw, and were 1.5 mm wide, with a 1 mm root radius. The notch form was of the triangular bridge type removing half the cross-section for most experiments, notable exceptions being the experiments described in Section 3.1.2. (variations in notch geometry). Unless otherwise stated, all tests were carried out on laboratory dried material, in air, at room temperature and at a cross-head displacement rate of 0.5 mm min$^{-1}$. The appearance of typical machine curves for stable, intermediate and unstable fracture are shown in Fig. 3. The decision as to whether a failure under conditions approaching instability was, in fact, still stable or not was a subjective one, based generally upon whether a break in the smooth curvature of the machine trace could be detected visually. The most usual place for this to be found was after the point of inflection following failure (see Fig. 3). In all cases, however, tests in which the complete stability of the fracture was in doubt were not included in the results used for obtaining the "mean value of fracture energy" for the particular rock, although they were retained for other purposes (e.g. in establishing close limits to the stability boundary).

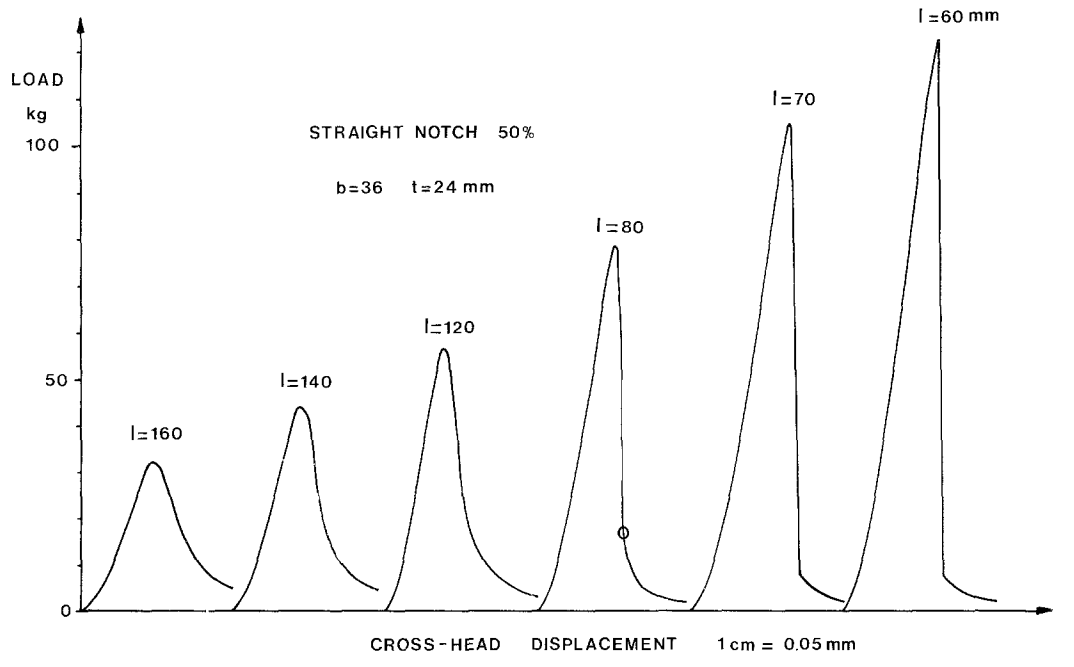


*Figure 3* Machine curves showing the transition from stable to unstable fracture.

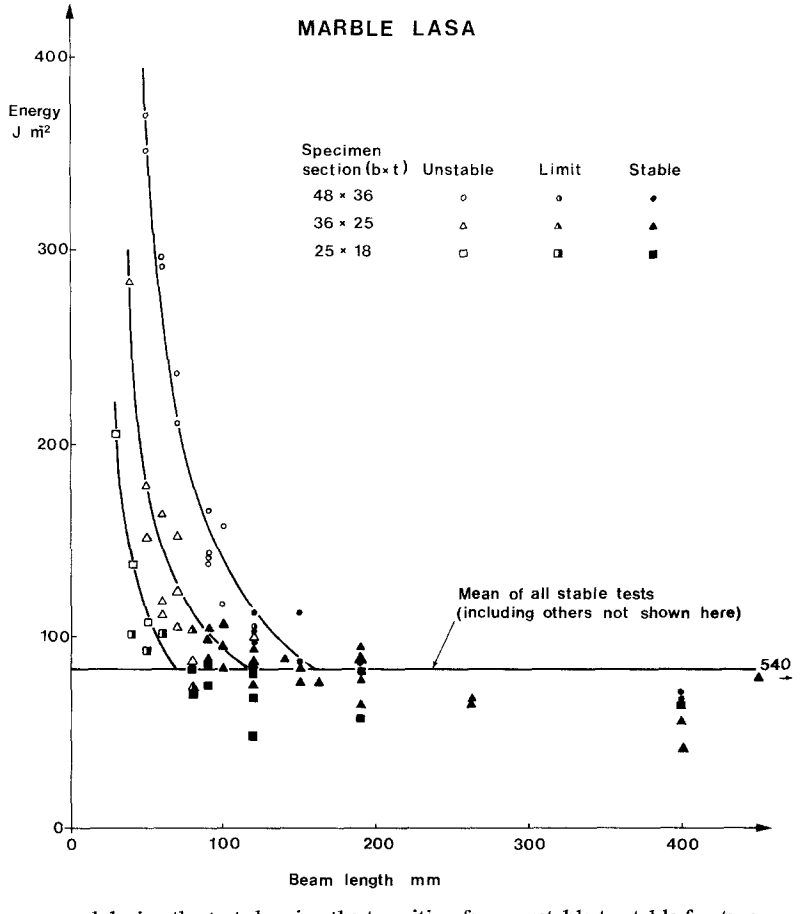


*Figure 4* Energy consumed during the test showing the transition from unstable to stable fracture.

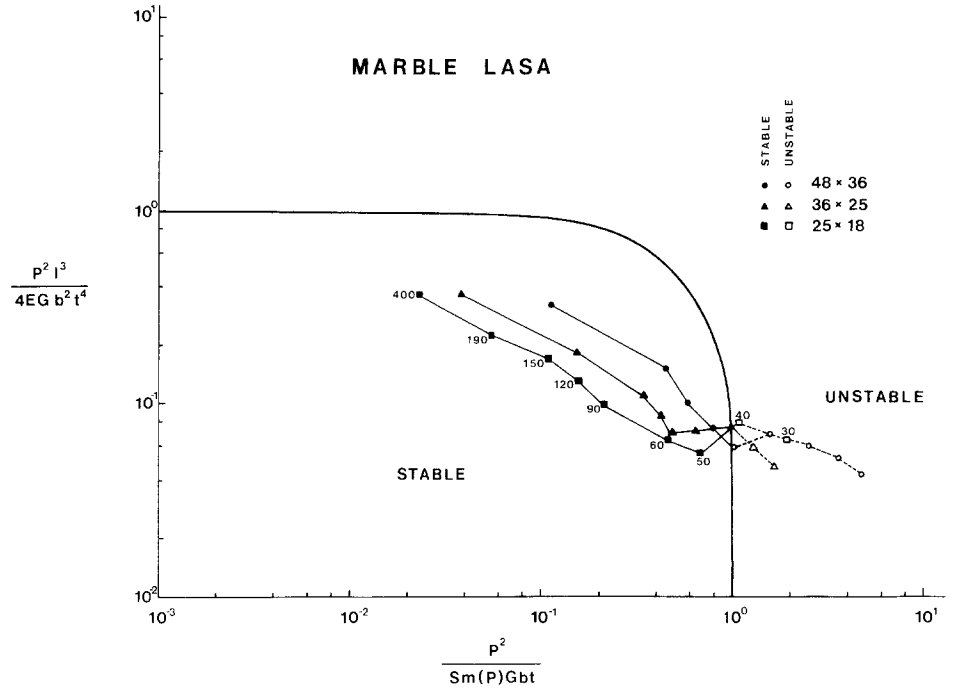


*Figure 5* Results obtained for three groups of beams of different cross-sectional area: lines join points for beams of the same cross-sectional dimensions but different length.

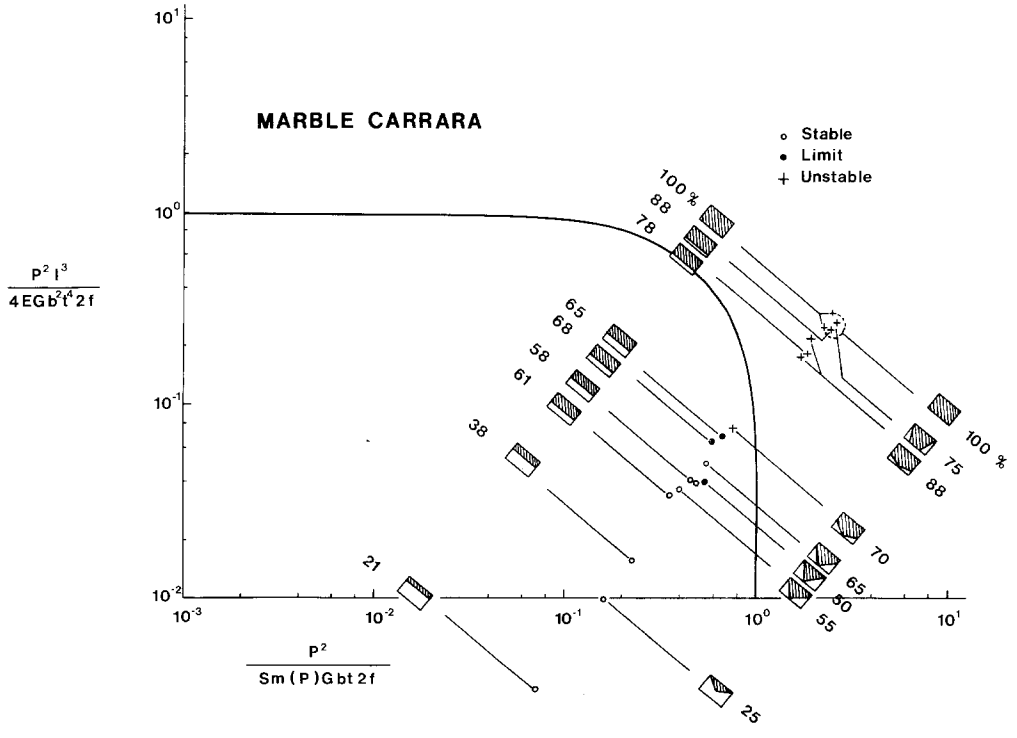


*Figure 6* The effects of varying notch geometry.

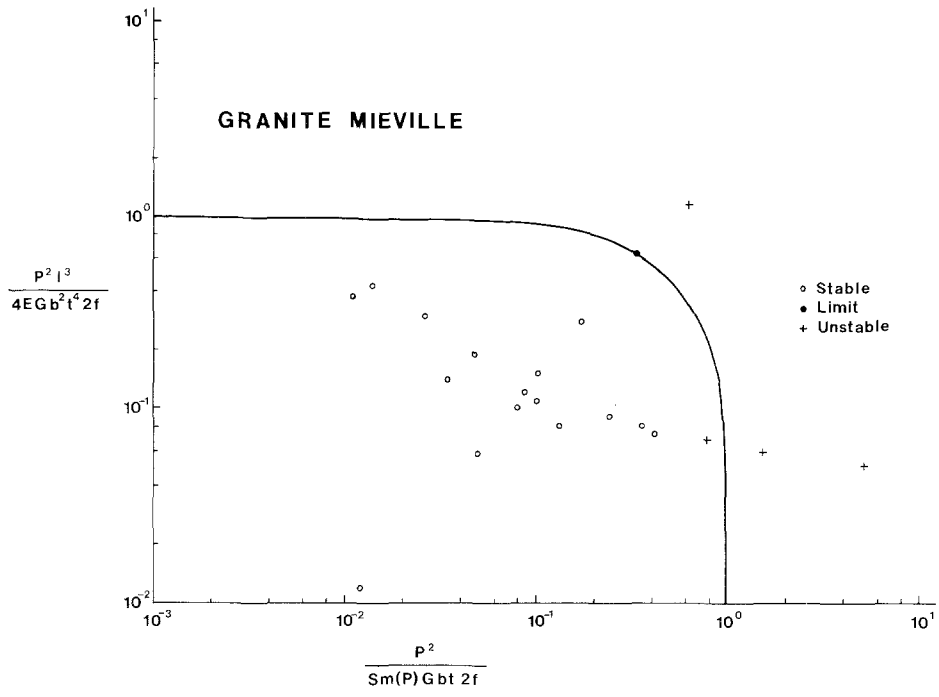


*Figure 7* Results for Miéville granite.

The effect of proximity to the boundary is shown in Fig. 4, where the "apparent fracture energy", taken as the area under the failure curve, is plotted against specimen length for specimens of Lasa marble of three different cross-sectional areas. For short specimens, up to nearly five times the energy necessary to produce the fracture was stored elastically before failure, and so under these conditions, the fracture was necessarily unstable. As the specimen length was increased, however, the stored elastic energy decreased until, in the region where the stored energy per unit area of potential fracture surface was near $100\,J\,m^{-2}$, stable fractures began to occur. For still greater specimen lengths, under conditions of stable fracture, the apparent fracture energy remained constant within the limits of variability normally found with this material. These values were then taken to be measures of the true fracture energy.

The validity of the stability criterion was examined by performing experiments in which systematic variations were made in the cross-sectional area, the length, the severity of the notch, and the type of rock. The fracture was observed to be stable or unstable, and was compared with the prediction of the stability criterion. The results are presented graphically, in terms of plots of $P^2l^3/4EGb^2t^4$ against $P^2/S_mGbt$ (dimensionless groups $A$), and the criterion is shown as a curved line separating stable (lower left) from unstable (upper right) conditions (see Figs. 5 to 10).

At an early stage in the evaluation of the results, apparent disagreements were found between theory and experiment. It was soon realized, however, that this was due to a non-linearity in the elastic response of the testing machine, causing the apparent machine stiffness to increase from $1.35 \times 10^6\,kg\,m^{-1}$ at 10 kg load to $3.7 \times 10^6\,kg\,m^{-1}$ at 500 kg load (Fig. 11). When the value of $S_m$ was chosen appropriate to the failure load of the specimen under test, however, these discrepancies were eliminated.

### 3.1.1. Variation of specimen dimensions

Fig. 5 shows results on three series of nine specimens of Lasa marble, of cross-sectional dimensions 48 mm x 36 mm, 36 mm x 25 mm and 25 mm x 18 mm, the breadth always being greater than the thickness. In each series, the nine lengths were 400, 190, 150, 120, 90, 60, 50, 40 and 30 mm.

When the results are reduced to the two dimensionless groups and plotted as described above, they fall into three parallel bands trending from upper left to lower right as the specimen length is decreased. The upper band corresponds to specimens with the greatest cross-sectional area, and the

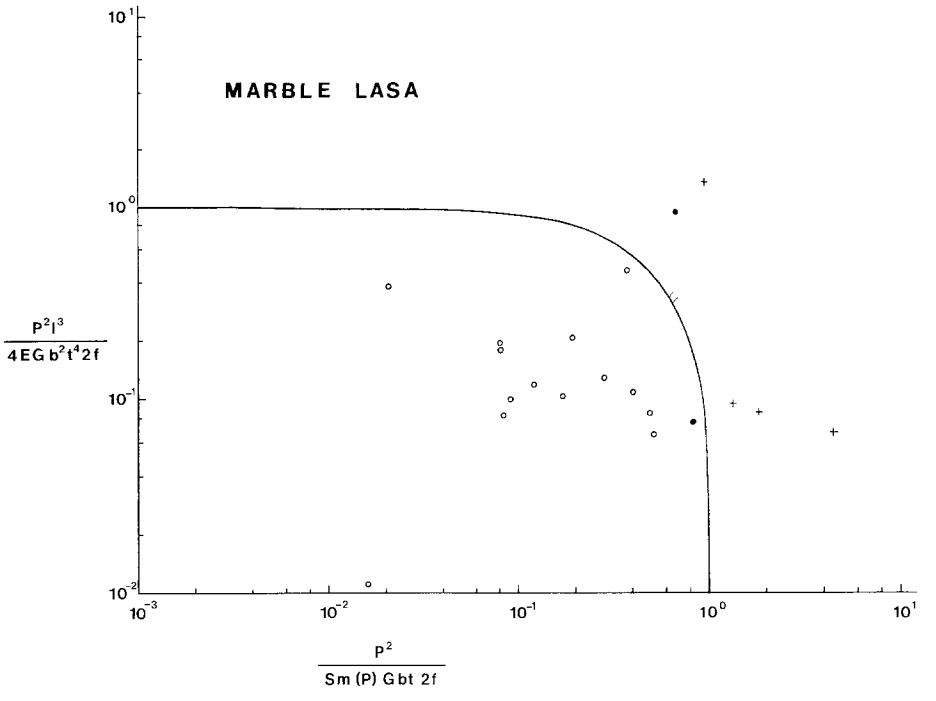


*Figure 8* Results for Lasa marble.

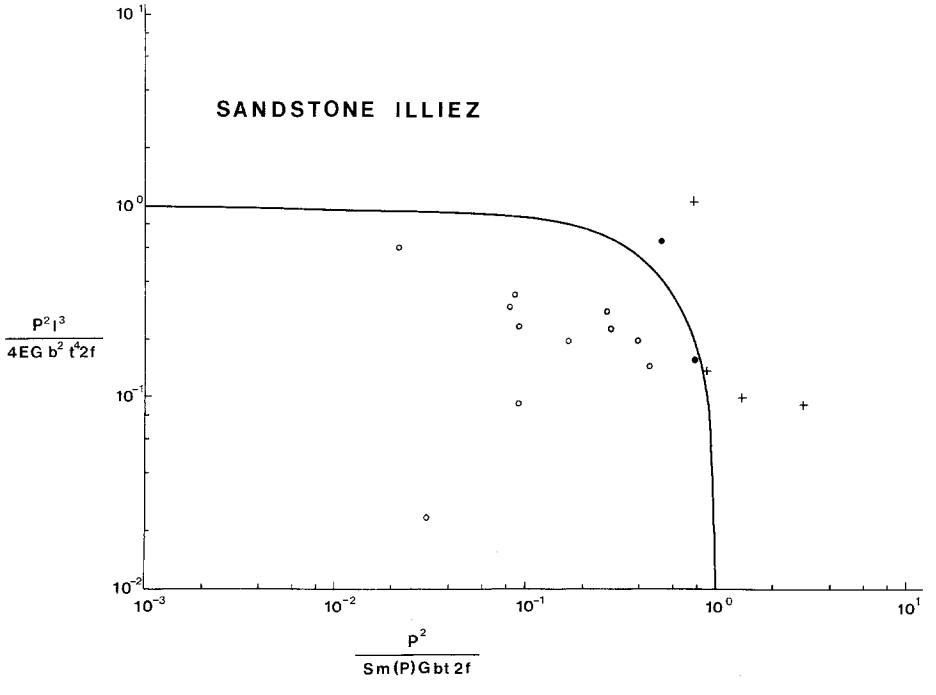


*Figure 9* Results for Val d'Illiez sandstone.

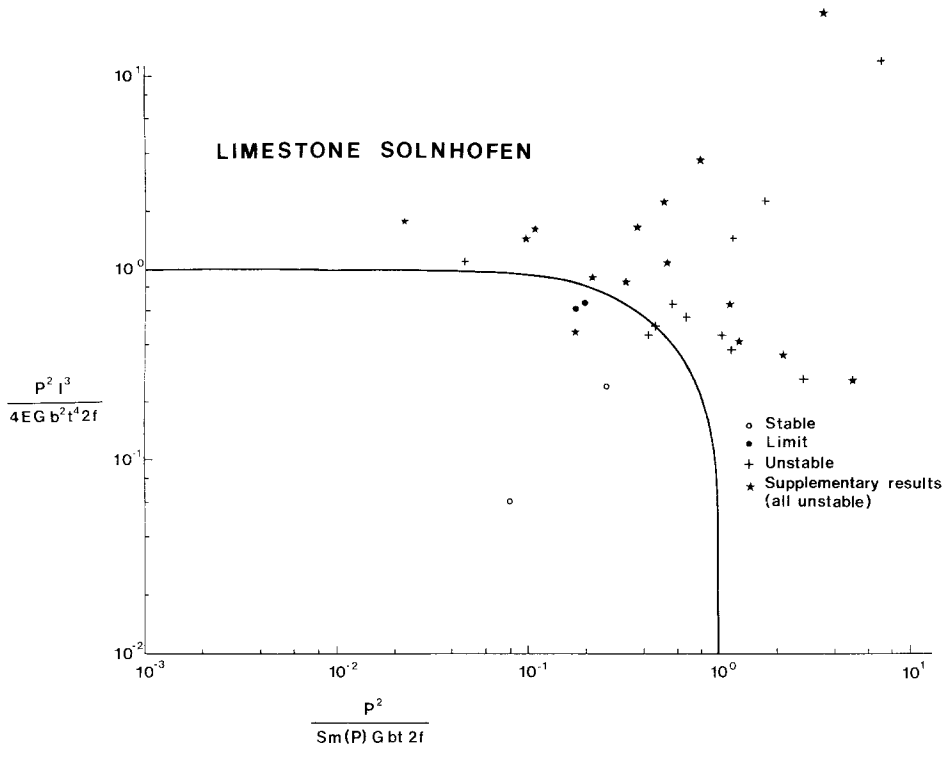


*Figure 10* Results for Solnhofen limestone.

lower to those with the least. Of particular interest is that when the beam length is reduced sufficiently for unstable fractures to be produced, points representing these specimens fall consistently and exclusively outside the stability boundary predicted by the theory.

Inspection of the graph indicates that it should also be possible to cross the instability boundary in the other direction (i.e. in testing very long specimens), but calculation showed that specimens of more than a metre long would have been required, and this dimension exceeded the maximum dimension of any of our pieces of raw material. The conclusion drawn from these experiments was, therefore, that the stability criterion was perfectly obeyed within the limits examined.

### 3.1.2. Variation of notch geometry

The next series of experiments was aimed at investigating the influence of notch severity and

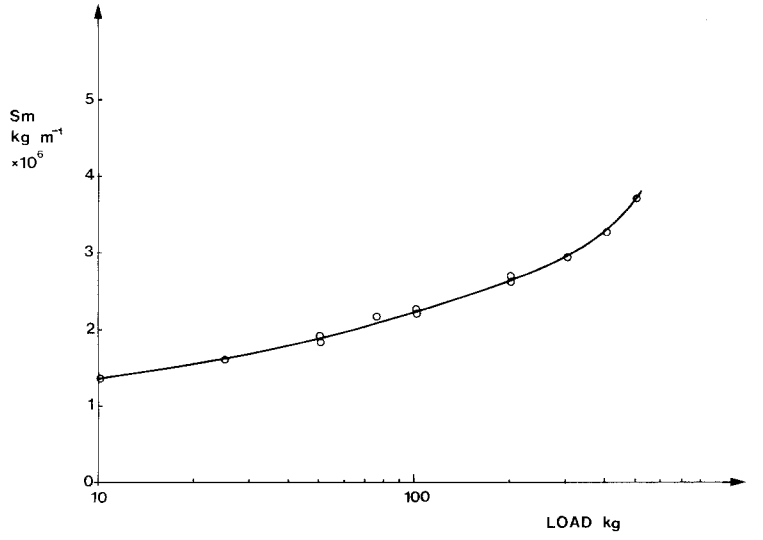


*Figure 11* Machine stiffness as a function of load.

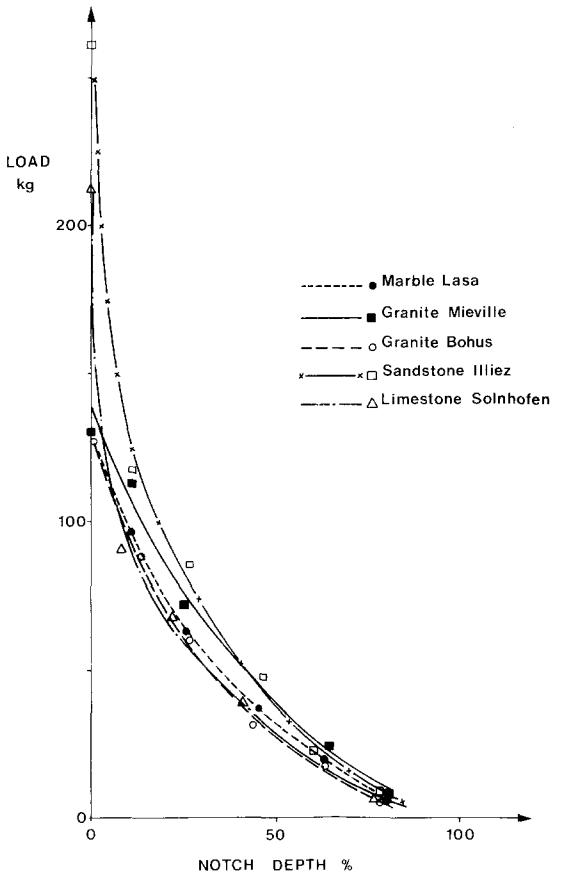


*Figure 12* Notch-sensitivity of different rocks.

geometry, using specimens of Carrara marble. In preliminary experiments, the variation of failure load with notch depth had been briefly investigated for straight notched specimens. Fig. 12 shows this variation: the degree of concavity of any curve is a measure of the notch-sensitivity of the material (deviation from the linear relation: failure load proportional to fraction of cross-sectional area remaining). It is worth noting that Solnhofen limestone clearly shows a greater degree of notch sensitivity than the other rocks, in complete agreement with its measured fracture energy, which is markedly less than the other rocks (see Section 3.3).

Altering the depth and shape of notch, therefore, forms a convenient method of changing the failure load and hence the stored elastic energy at failure. Specimens of constant dimensions 70 mm x 36 mm x 24 mm were prepared, with either straight notches of various depths, or variants of the "triangular bridge" type. The results were again reduced to dimensionless form, and are shown in Fig. 6. In making the calculations, it was necessary to introduce a factor $2f$ into the denominator of each group, to allow for the fact that the area of potential fracture surface alters with the form of the notch. $f$ has the value 1 for an unnotched beam, and 0 for the case where the notch cuts the beam completely in two. Again, inspection of Fig. 6 shows that the stability criterion is well obeyed, with only one exception.

### 3.1.3. Validity of the criterion of different rocks

The next series of tests was made to investigate whether the type of rock has any influence. Here, the main variable was the fracture energy, although the stiffness also varies from rock to rock, but to a lesser extent.

Figs. 7 to 10 show results for four rock types. All the tests were made on beams of 36 mm x 25 mm cross-section except for the Solnhofen limestone where both 36 mm x 25 mm and 25 mm x 16 mm sections were used. To obtain intersections with the stability boundary, some tests were made while varying the beam length with constant cross-sectional dimensions and notch, and some tests were made with constant beam length but with notches of differing severity. As we have seen above, the former procedure gives a trend from upper left to lower right, while the latter produces the opposite tendency on the dimensionless plot.

The results for the granite call for no comment except to note one unstable result on the wrong side of the boundary. The marble and sandstone results are well behaved also, and are very similar to the granite, but the results for Solnhofen limestone are distinctly different, for although the tests on specimens with varying notch depth gave a good traverse of the stability boundary, the tests with the standard notch form and beam dimensions proved to be nearly all unstable. Of all these tests, only two semi-stable results were obtained for a pair of tests under similar conditions and predicted to lie in the stable zone. A further group of tests was therefore undertaken, using thinner beams (25 mm x 16 mm) since it had been observed that, with the tests described in Section 3.1.1, on Lasa marble, thinner beams tended to give more stable results (see Fig. 5). These supplementary results are also shown in Fig. 10, but, as is seen, no more success was achieved in obtaining stability.

Upon completion of these tests, it was decided that the stability criterion had been sufficiently examined, since no general exception had been found for any of the parameters tested, and only a few individual tests had been found to fall contrary to prediction.

The severity of the examination perhaps leaves a little to be desired, but this is a consequence of the nature of the experiment; the transition from stable to unstable behaviour is not sharp, and it is extremely difficult experimentally in borderline cases to decide whether a fracture is to be regarded as stable or unstable. In any case, the value of the criterion is to be seen not as a means for approaching ever closer to the stability boundary, but to enable one to stay well away from it, in conditions which will give stable fractures in spite of minor experimental variations.

## 3.2. Effects of specimen size on fracture energy

The existence of a "size effect" on the fracture energy of rocks may be expected intuitively by noting that the fracture energies of most rocks are about two orders of magnitude greater than those of single crystals of the minerals from which they are formed [10], a phenomenon which is supposed to stem from the polycrystalline nature of the rocks, causing irregular and sometimes multiple fracture paths. The effects of irregularity have been estimated by Hoagland *et al.* [18], who have shown that the true fracture area may be more than an order of magnitude greater than the apparent area, with consequent direct influence on the fracture energy. In addition, if multiple (parallel) fracture occurs, if microcracks are produced in the region of the crack tip which do not form part of the final fracture surface, or if frictional losses occur in separating interlocking groups of crystals, the fracture energy will be even further increased.

As the specimen size is decreased, however, these effects should become less important. Ultimately, of course, as the specimen cross-sectional area reduces to less than that of a single grain, one should be able to measure a fracture energy no greater than that for cleavage of the single crystal.

With this idea in mind, therefore, a series of tests was made on Bohus granite and on Lasa marble, varying the cross-sectional area from nearly 3000 $mm^2$ down to as little as could be achieved with the specimen preparation techniques at our disposal. This was 2 $mm^2$ (2 mm x 2 mm, half the section being removed by notching) and 8 $mm^2$ (4 mm x 4 mm) for the granite, which

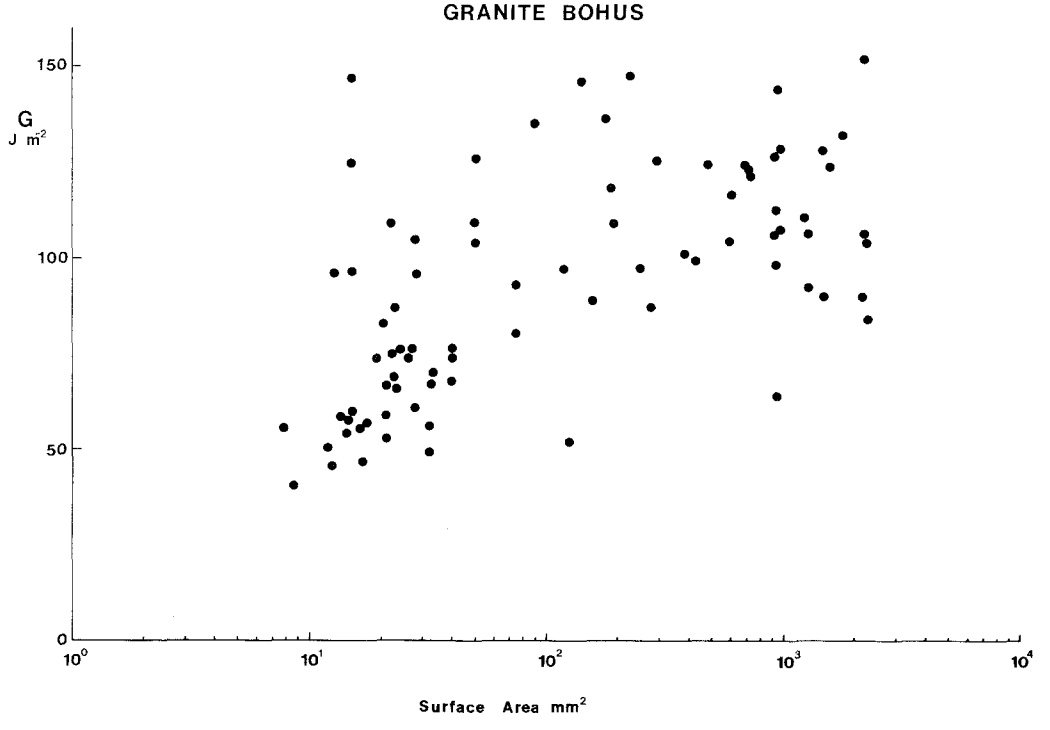


*Figure 13* Apparent fracture energy as a function of specimen cross-sectional area: Bohus granite.

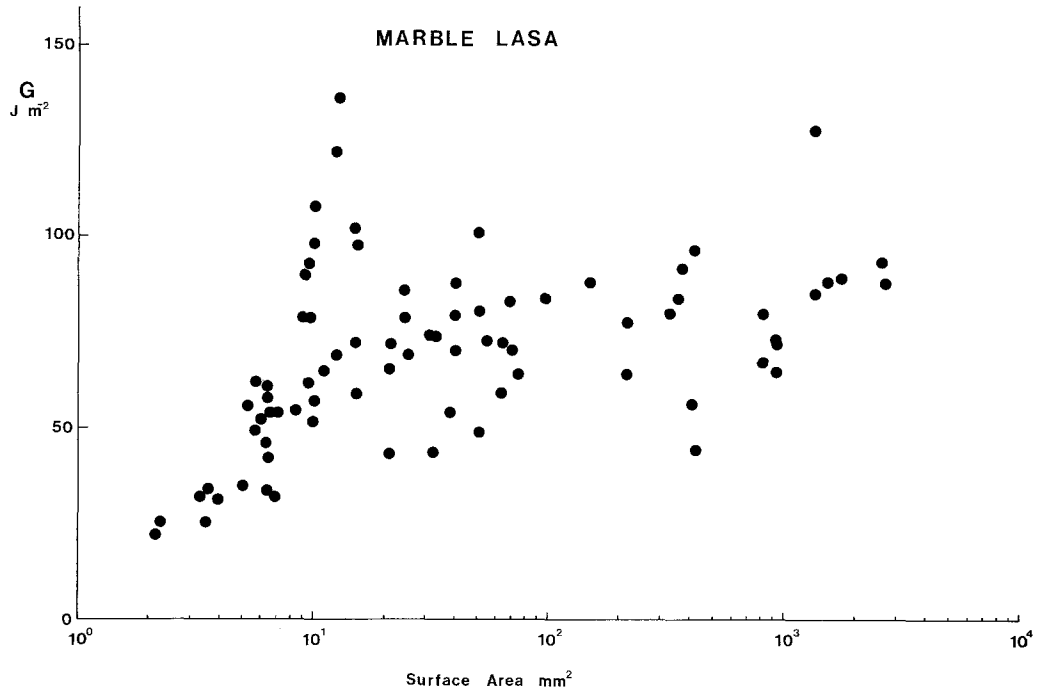


*Figure 14* Apparent fracture energy as a function of specimen cross-sectional area: Lasa marble.

tended to break more easily during sawing. The cross-sections were maintained with the breadth either equal to or somewhat larger than the thickness, and the length was chosen to give an optimum chance of stability, within the dimensions available from the raw material.

The results obtained are shown in Figs. 13 and 14. In both cases, there seems to be a distinct downward trend for small specimens. In the case of the marble, it is noticeable in the region of $20\,mm^2$, and for the granite, in the region of $10\,mm^2$. In both of these rocks, the grain size is of the order of 2 mm although the granite has a broader distribution of grain size. Fracture in a specimen of $20\,mm^2$ thus involves a half-dozen or so grains. It is quite reasonable, therefore, that at this size there should be a distinct trend from the properties of the mass towards those of the single crystal. From the point of view of the present work, however, the most important point is that there appears to be no size effect in the range 200 to $1000\,mm^2$, where most of the testing of the fracture criterion has been carried out. We are therefore confident that the values of fracture energy measured in the main series of experiments are representative of the rock in bulk.

TABLE I Collected fracture energies for rocks

| Rock type | $G$ ($J\,m^{-2}$) | Standard deviation | Number of tests |
|---|---|---|---|
| Marble Lasa | 82 | 16 | 79 |
| Marble Carrara | 71 | 13 | 9 |
| Sandstone Alpnach | 94 | 12 | 23 |
| Sandstone Val d'Illiez | 98 | 15.0 | 15 |
| Granite Bohus | 116 | 26 | 57 |
| Granite Miéville | 193 | 30 | 19 |
| Limestone Solnhofen | 24 | 2 | 4 |

## 3.3. The absolute values of the fracture energy

The values of fracture energy obtained from all our tests are given in Table I. It will be seen that the values vary quite widely, from somewhat more than $20\,J\,m^{-2}$ for Solnhofen limestone to nearly $200\,J\,m^{-2}$ for the Miéville granite. These values do not appear to be related to the compressive strength of these rocks, but there is a rough correlation with the grain size. The Miéville granite is

quite coarse-grained, having individual crystals up to several millimetres across, while the limestone is extremely fine-grained, with grains only rarely exceeding 100 $\mu$m; between, with intermediate grain sizes lie the Bohus granite, the sandstones and marbles, although it should be noted that both the marbles are somewhat coarser grained than the sandstones.

## 4. Conclusions

The purpose of this report has been to present a simple and straightforward means for determining under what conditions it will be possible to obtain valid values of the fracture energy from a given material in a given machine using the normal three point bend test on a notched beam. The analysis has been presented as straight forwardly as possible, the main purpose being not to exactly determine the stability boundary, but to provide a simple indication which will help in designing experiments which are well within the stable region.

The experimental results reported confirm the predictions of the criterion very well, and show how in a typical testing machine it is possible to obtain either valid or invalid measures of the fracture energy by relatively small changes in the specimen dimension.

## References


1. R. L. BERTOLETTI, *J. Amer. Ceram. Soc.* 57 (1974) 300.
2. G. P. MARHSALL, J. G. WILLIAMS and C. E. TURNER, *J. Mater. Sci.* 8 (1973) 919.
3. H. G. TATTERSALL and G. TAPPIN, *ibid* 1 (1966) 296.
4. R. W. DAVIDGE and G. TAPPIN, *ibid* 3 (1968) 165.
5. J. NAKAYAMA, *J. Amer. Ceram. Soc.* 48 (1965) 583.
6. W. F. BROWN and J. E. SRAWLEY, ASTM special technical publication No. 410, ASTM Philadelphia (1966) p. 9.
7. G. C. SIH, "Handbook of stress intensity factors", (Institute of Fracture and Solid Mechanics, Lehigh University, Bethlehem. Pa., 1973).
8. R. G. HOAGLAND, G. T. HAHN, A. T. ROSENFIELD, R. SIMONS and G. D. NICHOLSON, Battelle research report, Contract HO 210006 January 1972).
9. R. G. HOAGLAND, G. T. HAHN, and A. R. ROSENFIELD, *Rock Mechanics* 5 (1973) 77.
10. J. J. GILMAN, *J. Appl. Phys.* 31 (1960) 2208.
11. H. BERGKVIST, to be published.


Received 11 May and accepted 2 June 1976.